Xylene Isomerization Using Zeolites in a Gradientless Reactor System

A gradientless reactor was used to study the xylene isomerization reaction over a series of cation-exchanged (H^+, Li^+, Na^+, and K^+) ultrastable faujasite and on ZSM5 and silicalite to observe the effects of site modification on the reaction. Adsorption, diffusion, and kinetic parameters were determined in the presence of the reaction; the results generally agreed with the available literature data. The gradientless reactor and associated modeling techniques are shown to be effective tools in investigating catalyst behavior. Precise analytical techniques are required to directly measure the diffusion coefficient in the presence of reaction.

Y. H. Ma and L. A. Savage
Department of Chemical Engineering
Worcester Polytechnic Institute
Worcester, MA 01609

Introduction

In the design of commercial-scale reactors employing porous heterogeneous catalysts, the knowledge of kinetic, adsorption, and diffusion effects is critical for successful scale-up from laboratory or pilot plant reactors. Experimental measurements of intrinsic reaction rate, adsorption equilibrium constant, and diffusion rate can be used with mathematical models of catalytic reactors to help improve the reliability of the reactor design. A simple yet accurate laboratory technique for obtaining such data could reduce extensive pilot plant testing while also allowing for evaluation of a wider range of alternative catalyst materials.

Often the fixed-bed reactor is used as a tool for obtaining catalytic reaction parameters; however, many difficulties may be encountered. Concentration and/or temperature gradients occur within the flowing phase of the catalyst bed and, while the measurements or mathematical modeling can be used to describe the gradients, such efforts can interfere with the determination of the desired intraparticle parameters. The differential reactor and pulsed microreactor have been applied to the study of porous catalysts, but analytical problems due to small conversion levels have been identified and minimization of the bulk phase gradients may not be assured (Carberry, 1964).

To help alleviate the problems associated with fixed-bed reactors, the spinning catalyst bed reactor (or "gradientless" reactor) was developed (Carberry, 1964; Brisk et al., 1968; Choudhary and Doraiswamy, 1972). In this design, the catalyst bed is attached to a rotor that spins the catalyst at high speed within the bulk phase, thus providing flow through the catalyst to minimize concentration and temperature gradients while also stirring the bulk phase. The reactant or product concentrations determined at the reactor effluent, and the temperature of the well-stirred bulk phase, should represent the prevailing conditions at the outside surface of each catalyst particle. These measurements can then be used to investigate the relevant intraparticle phenomena.

Many of the available literature studies concerning heterogeneous catalysis in zeolites have utilized fixed-bed reactors and have concentrated on a single phenomenon relevant to the catalyst behavior. Equilibrium adsorption of one or more components on zeolites has been studied mainly through the use of gravimetric or volumetric measurements of sorbent uptake using microbalances or precision volumetric methods (Breck, 1974) to obtain adsorption isotherms. Dynamic methods have also been attempted in which pulse techniques are applied to either a fixed bed (Ma and Mancel, 1972; Chiang, 1982) or a stirred tank (Santacesaria et al., 1982) using mathematical models similar to those of gas chromatography. These dynamic methods can be used to obtain effective diffusion coefficients in addition to linear equilibrium constants for adsorption. Diffusion in zeolites has also been studied by measuring the kinetics of adsorption in equipment similar to that used for equilibrium adsorption measurements, and applying a mathematical model of concentration gradients within the zeolite crystal to the experimentally determined sorbent uptake vs. time curves (Barrer, 1980). In most instances these studies are carried out at temperatures lower than that required for reaction, and temperature extrapolations of equilibrium and diffusion constants are performed to utilize the data in the reaction regime. There is no

L. A. Savage is currently with Cabot Corporation, Billerica, MA.

assurance that such extrapolations are valid, especially if competitive adsorption or counterdiffusion of product species occurs at reaction temperatures.

Few studies have attempted to measure adsorption and diffusion parameters during reaction over a zeolite catalyst. The amount of reactant adsorbed during zeolite-catalyzed hydrocarbon reactions can be small due to both the high temperatures employed and possible competitive adsorption of product species. Although adsorption and reaction have been studied in fixed beds of zeolite catalysts using gas chromatographic techniques (Bassett and Habgood, 1960; Bartley et al., 1968) diffusion parameters were not included in these analyses. However, through the use of a gradientless reactor, the mathematical modeling of adsorption, diffusion, and reaction can be performed. Ma and Schobert (1981) have applied these techniques to the isomerization of cyclopropane with faujasite catalysts.

The purpose of this study was to investigate orthoxylene isomerization over ZSM-5, silicalite, and ultrastable faujasite catalysts using the gradientless reactor and mathematical modeling to determine kinetic, adsorption, and diffusion parameters in the presence of reaction. These parameters provide insight into the nature of zeolite catalysis and the properties of the active site which previously have been difficult to study in the presence of reaction.

Mathematical Model

In the analysis of the gradientless reactor, Laplace transform techniques and the method of moments are applied to the partial differential equations governing catalyst behavior. Further details of these derivations are available in Ma and Schobert (1981). In this work only catalyst beds of powdered zeolite crystals (micropore model) have been considered and the following assumptions have been made.

1. As shown in Figure 1, within the reactor there are three regions where a reactant molecule may exist. The gas phase, Y, surrounds the catalyst particles and is well stirred by the spinning catalyst bed. A mobile intracrystalline phase, C_i, is present in the zeolite's pores, and diffusion within this phase is described by Fick's law with constant diffusion coefficient. An adsorbed phase, C_{si}, exists on the internal surface of the micropores and reaction occurs only in this layer.
2. The catalyst particles are spherical and uniform.
3. The reaction is irreversible, and first-order kinetics apply.
4. The adsorption equilibrium isotherm is linear within the region of interest and the temperature is uniform throughout the catalyst.

Material balances in the form of partial differential equations can be derived for each of the three phases described above.

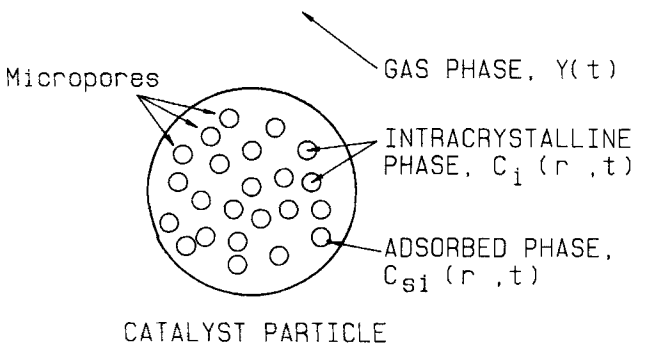

Figure 1. Catalyst particle and three phases where reactant molecules may exist

Gas Phase

$$V\frac{dY}{dt} = F(X - Y) - D_i 4\pi R_i^2 N \epsilon_i \left.\frac{\partial C_i}{\partial r_i}\right|_{r_i = R_i} \tag{1}$$

Adsorbed Phase

$$\frac{k_a \epsilon_i}{A_v}\left(C_i - \frac{C_{si}}{K_p}\right) - k_s C_{si} = \frac{\partial C_{si}}{\partial t} \tag{2}$$

Intracrystalline Phase

$$\frac{D_i}{r_i^2}\left[\frac{\partial}{\partial r_i}\left(r_i^2 \frac{\partial C_i}{\partial r_i}\right)\right] - k_a\left(C_i - \frac{C_{si}}{K_p}\right) = \frac{\partial C_i}{\partial t} \tag{3}$$

The corresponding boundary and initial conditions are:

$$\frac{\partial C_i}{\partial r_i}(0, t) = 0 \tag{4a}$$

$$C_i(R_i, t) = Y(t) \tag{4b}$$

$$C_i(r_i, 0) = 0 \tag{5a}$$

$$C_{si}(r_i, 0) = 0 \tag{5b}$$

$$Y(0) = 0 \tag{5c}$$

Since C_{si} and C_i are not readily determined experimentally, Eqs. 1, 2, and 3 are solved with Laplace transform techniques in terms of $\tilde{Y}(S)$ because $Y(t)$ may be measured at the reactor effluent.

$$\frac{\tilde{Y}(S)}{\tilde{X}(S)} = \left[1 + \tau S + 2\tau_i \epsilon_i \frac{D_i}{r_i^2}(\alpha(S)\coth\alpha(S) - 1)\right]^{-1} \tag{6a}$$

$$\alpha(S) = \frac{R_i}{(D_i)^{1/2}}\left(S + k_a - \frac{k_a^2}{K_a S + K_a k_s + k_a}\right)^{1/2} \tag{6b}$$

$$\tau_i = \frac{v_i}{F} = N\frac{4\pi R_i^3}{3F} \tag{6c}$$

Inversion of Eqs. 6a, b, c is difficult but the method of moments may be applied. By taking the nth derivative of $\tilde{Y}(S)$ followed by the limit as $S \to 0$, the nth moment of $Y(t)$ may be obtained.

$$\lim_{S\to 0}\frac{\delta^n}{\delta S^n}\left[\int_0^\infty e^{-St}Y(t)\,dt\right] = (-1)^n\int_0^\infty t^n Y(t)\,dt \tag{7}$$

This is done for $n = 0$, 1, 2, and the moments of $Y(t)$ thus determined, M_i, are grouped according to convenient character-

istic functions: I, I', I''.

$$I = \frac{1}{M_O} = 1 + \frac{v_i}{F}\epsilon_i K_a k_s \eta_i \tag{8}$$

$$I' = \frac{M_1}{M_O^2} = \tau + \frac{3}{2}\frac{v_i}{F}\epsilon_i(1 + K_a)P(\phi_i) \tag{9}$$

$$I'' = \frac{M_1^2}{M_O^3} - \frac{M_2}{M_O^2} = \frac{3}{4}\frac{v_i}{F}\epsilon_i \frac{R_i^2}{D_i}(1 + K_a)^2 Q(\phi_i) \tag{10}$$

Defining:

$$\eta_i = \text{effectiveness factor} = (3/\phi_i)(\phi_i \coth \phi_i - 1) \tag{11a}$$

$$\phi_i = \text{modified Thieles modulus} = (R_i^2 K_a k_s / D_i)^{1/2} \tag{11b}$$

$$P(\phi_i) = [(\cosh \phi_i)(\sinh \phi_i) - \phi_i]/\phi_i \sinh^2 \phi_i \tag{11c}$$

$$Q(\phi_i) = [2\phi_i^2 \cosh \phi_i - \phi_i \sinh \phi_i - \cosh \phi_i \sinh^2 \phi_i]/\phi_i^3 \sinh^3 \phi_i \tag{11d}$$

These particular groupings of the experimentally determined moments are helpful in that each characteristic function is linear with the inverse gas flow rate. By performing experiments at different flow rates, the slopes and intercepts of the characteristic functions determined by linear regression techniques are used to evaluate the model parameters, K_a, k_s, D_i.

In the case when diffusion is not rate controlling, the function I'' tends toward zero and the model can be simplified to consider only adsorption and reaction. Equations 8 and 9 become:

$$I = \frac{1}{M_O} = 1 + \frac{v_i}{F}\epsilon_i K_a k_s \tag{12}$$

$$I' = \frac{M_1}{M_O^2} = \frac{V}{F} + \frac{v_i}{F}\epsilon_i(1 + K_a) \tag{13}$$

The model parameters K_a and k_s are easily obtained by simple linear regression analysis in this instance.

Experimental Apparatus

A diagram of the gradientless reactor system is shown in Figure 2. Helium carrier gas was continuously supplied to the reactor from a gas cylinder by first passing the helium through Drierite and molecular sieve adsorbent beds to remove water. A needle valve was used to control helium flow, while a rotameter indicated the volumetric flow rate prior to introduction of the gas into the reactor at atmospheric pressure. The stainless steel reactor vessel had a volume of $3.5 \times 10^{-3}\text{m}^3$ which was stirred by the rotation of the two cylindrical catalyst beds. The beds consisted of wire mesh baskets fixed to a rotor which was spun at 3,600 rpm by a magnetically coupled drive. Powdered catalyst was suspended in glass wool and accurately weighed before being placed in the wire baskets. Heating was provided by electric cartridge heaters that also acted as baffles to mix the gas while temperature was controlled to within 1°C through a feedback loop. Reactor effluent flowed through low-volume tubing

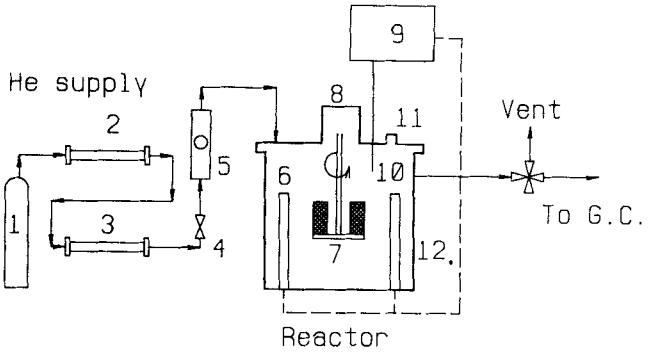

Figure 2. Gradientless reactor configuration.

1. Helium cylinder
2. Drierite bed
3. Molecular sieve bed
4. Flow control valve
5. Rotameter
6. Electric cartridge heater
7. Catalyst baskets
8. Magnetically coupled drive
9. Temperature controller
10. Thermocouple
11. Injection port
12. Reactor shell

to a multiposition valve that allowed the gas to be vented or passed to the gas chromatograph for analysis.

A run was performed by first dehydrating the catalyst at 620 K (about 1.3 g) for 3 h under a small flow of helium. The rotor was then set spinning and reactor temperature set at the desired level while at least 15 min was allowed for stabilization. To begin the reaction about 4μL of liquid orthoxylene was injected directly into the reactor through a septum in the reactor lid. The first gas chromatograph (GC) sample was taken at t = 10 s by using a ten-port gas sampling valve in the reactor effluent line, and sampling continued each minute thereafter until xylene concentrations fell by at least a factor of 100 (approx. 10 min).

Tracer experiments were performed to determine if the reactor was truly well mixed. The catalyst beds were emptied and orthoxylene was injected through the septum at t = 0 s. GC analysis measured orthoxylene concentration as a function of time at the reactor effluent in the same manner described above. In all cases, semilog plots of orthoxylene concentration vs. time showed good linearity, while the calculated slopes ($-1/\tau$) provided reactor residence times within 10% of residence times calculated by direct methods (measured reactor volume/gas flow rate). This indicated that the gas within the reactor was well mixed and little dead space was present. Also, since the orthoxylene concentration measured at t = 10 s showed good agreement with the least-squares fit of all the data points, the liquid orthoxylene injected was completely vaporized in less than 10 s. No reaction products were detected in these tracer experiments, indicating that there is little contribution to the xylene isomerization from homogeneous reactions or wall effects.

Additional tests were performed to evaluate the extent of mass transfer between the catalyst particles and the gas phase. Pitot tube experiments were performed to measure gas velocity adjacent to the spinning rotor. Gas velocity was found to be much less than the tangential velocity of the rotor (2.1 vs. 8.5 m/s), indicating that there is little circulation of the gas phase with the rotor and that the fluid velocity relative to the catalyst particle is high. Using the relative fluid velocity in the mass transfer correlation of Brian and Hales (1969), one obtains a mass transfer rate many orders of magnitude greater than the fastest reaction rate measured in this study. While it is unlikely

that such correlations are accurate for small particles, the error in the extrapolation should not be many orders of magnitude and mass transfer rate should be significantly faster than the reaction rates measured. In addition, strong variations of reaction rate with temperature have also been observed (Savage, 1983) with activation energies of 54–121 kJ/mol. Such strong temperature variations are not indicative of gas phase mass transfer control. Since gas phase mass transfer coefficients vary only slightly with temperature, apparent activation energies less than 15 kJ/mol would normally be expected if mass transfer rate were controlling.

Catalyst preparation

Ultrastable faujasite (USY) was obtained in the NH_4^+-exchanged form and was converted to the H^+-exchanged form by calcining in air at 873 K for 48 h. Various ion-exchanged forms (Na^+, Li^+, K^+) were prepared to study the effect of cation size on model parameters. This was performed by slurrying the H^+ form in 1.0M nitrate solutions of the desired cation for a period of 1 h. The faujasite was then filtered and rinsed with distilled water. After repeating this procedure twice more, the zeolite was dried at 398 K. These powders were analyzed by atomic absorption spectroscopy and BET surface area measurement; the results appear in Table 1.

X-ray diffraction studies showed that the crystal structures were unaffected by the ion exchange, and SEM micrographs indicated that the average particle size was 2 μm in each cation form.

The ZSM-5 used in this study was also received in NH_4^+-exchanged form and this was converted to the H^+ form by calcination in air at 873 K for 48 h. SEM photographs were used to estimate an average particle size of 0.5 μm and BET surface area was 368 m^2/g.

The silicalite obtained for this study was calcined by the manufacturer after synthesis and no further treatment was required. Particle size was estimated at 1.5 μm and the BET surface area was measured at 400 m^2/g.

Results and Discussion

Reactions with ultrastable faujasite

A series of orthoxylene isomerization runs was performed on each of the ion-exchanged forms of ultrastable faujasite (H^+,Li^+, Na^+, and K^+) using a range of carrier flow rates at three different temperatures. The zero, first, and second moments of the reactor effluent response were calculated by numerically integrating the orthoxylene concentration decay curve and these moments were grouped according to the characteristic functions I, I', I'' shown in Eqs. 8–10. In runs with each ion-exchanged form, the value of the function I'' was close to zero, indicating that reactant molecules experienced little diffusion resistance that was measurable by this technique. In this case the degenerate model represented by characteristic functions I and I' in Eqs. 12 and 13 applied; typical plots of these functions for H-USY are shown in Figures 3 and 4. Similar plots were generated for Li-USY and Na-USY and each exhibited good linearity with inverse flow rate with appropriate intercepts;

Table 1. BET Surface Area and Chemical Analysis for Ion-exchanged Ultrastable Faujasite

	H-USY	Li-USY	Na-USY	K-USY
SA, m^2/g	656	633	632	—
Si, wt. %	24	24	22	24
Al, wt. %	8.2	7.6	6.9	7.6
Li, wt. %	<0.002	0.35	<0.002	—
Na, wt. %	0.1	0.2	2.0	0.008
K, wt. %	—	—	—	3.2

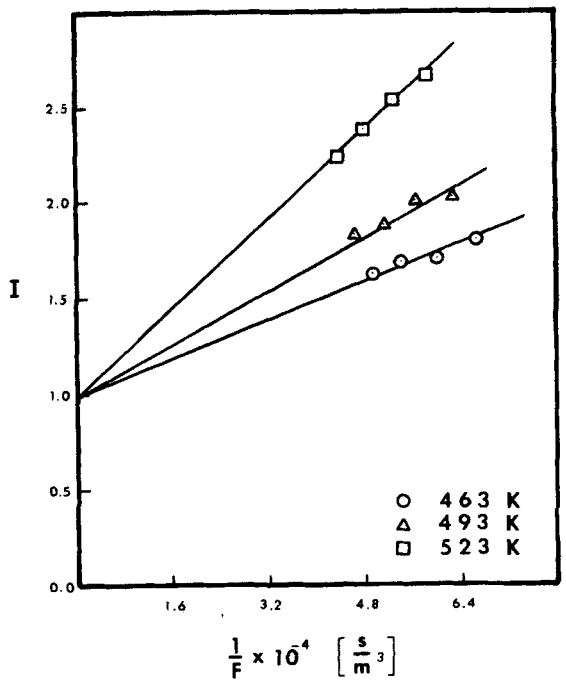

Figure 3. Function I vs. $1/F$ for hydrogen-exchanged ultrastable faujasite.

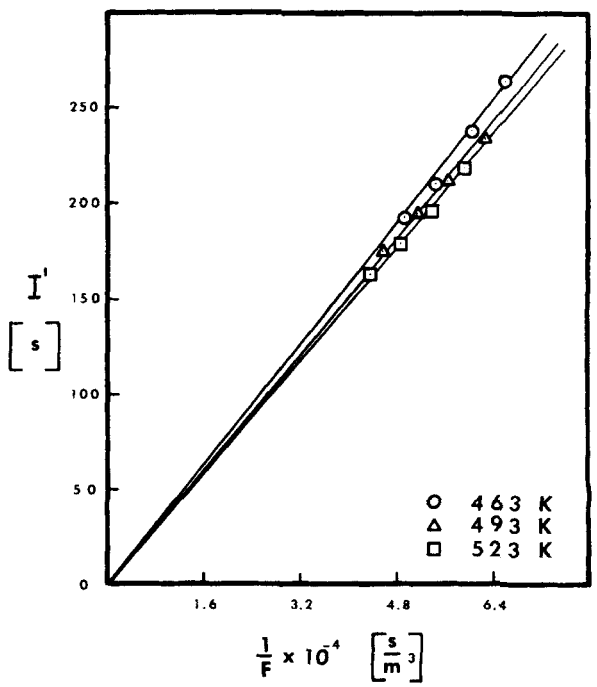

Figure 4. Function I' vs. $1/F$ for hydrogen-exchanged ultrastable faujasite.

Table 2. K_a and k_s for Ion-exchanged Ultrastable Faujasite

	Equilibrium Constant, K_a			Reaction Rate Constant, k_s (1/s)		
Temp. K	H-USY	Li-USY	Na-USY	H-USY	Li-USY	Na-USY
463	1,406	—	—	0.02	—	—
478	774	—	—	0.044	—	—
493	382	2,599	—	0.108	0.0103	—
523	116	1,523	2,567	0.72	0.0267	0.0086
548	—	615	1,629	—	0.0846	0.0156
573	—	—	1,376	—	—	0.0252

however, little reaction was observed with K-USY and no results are reported for this catalyst.

No diffusion resistance was expected in isomerization of orthoxylene in faujasite since the cage opening (0.9 nm) of the zeolite is somewhat greater than the kinetic diameter of o-xylene (0.6 nm) and this should allow good mobility of the reactant molecule through the crystal. Conservative estimates of diffusion rate through the small 2 μm particles used in this study (Savage, 1983) indicated that the rate of reaction would be at least 40 times slower than the rate of diffusion (see Supplementary Material) and the small values of I'' obtained from the moments confirm this.

From the slope and intercept values of the least-squares fit to the characteristic functions the model parameters k_s and K_a shown in Table 2 were determined for each ion-exchanged form of ultrastable faujasite.

From the temperature dependence of the model parameters further information was derived. The reaction rate constant data exhibited an Arrhenius-type dependence on temperature:

$$k_s = k_{so}e^{-E_a/RT} \tag{14}$$

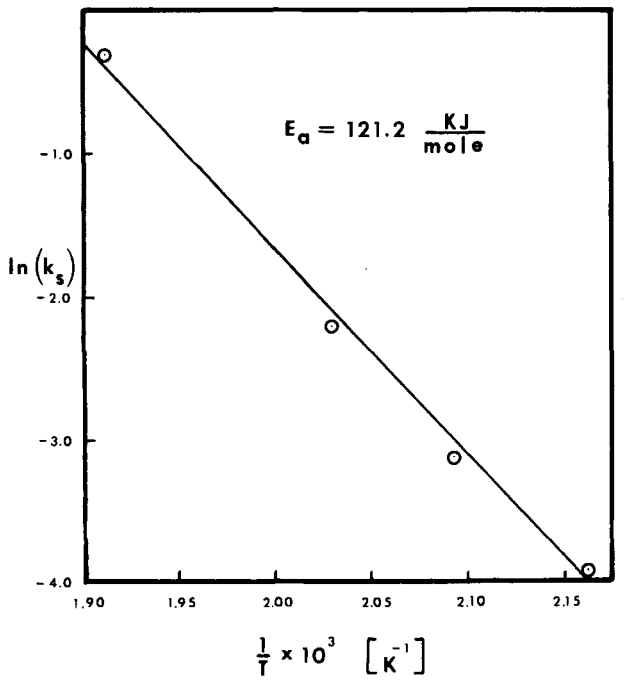

Figure 5. Arrhenius plot for H-USY showing ln (k_s) vs. $1/T$.

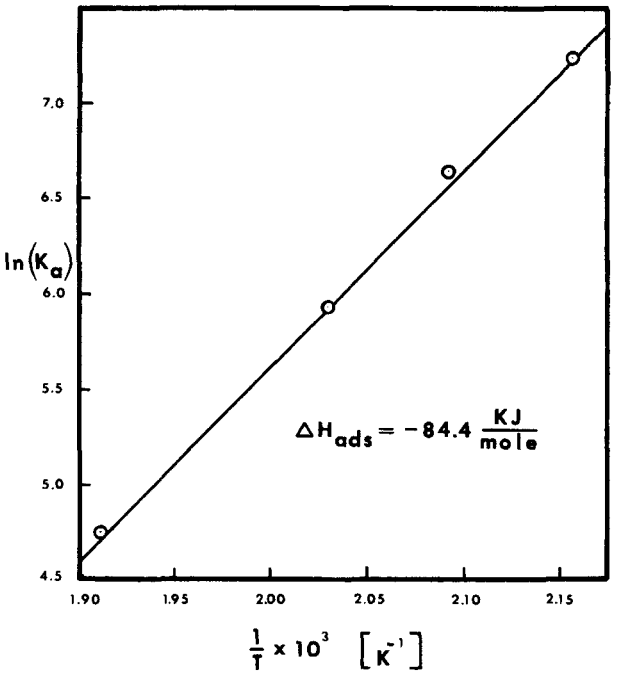

Figure 6. Van't Hoff plot for H-USY showing ln (K_A) vs. $1/T$.

The equilibrium constant data showed close agreement to the Van't Hoff law when ln (K_a) was plotted vs. inverse temperature.

$$\frac{d \ln (K_a)}{d(1/T)} = \frac{-\Delta H}{R} \tag{15}$$

Figures 5 and 6 demonstrate the close fit of the data for H-USY to the Arrhenius and Van't Hoff relationships that was also observed with each of the ion-exchanged forms. Table 3 contains the activation energy and heat of adsorption parameters determined by least-squares fit.

The linearity observed by the characteristic functions and the agreement of the model parameters with Arrhenius and Van't Hoff relationships provides some evidence that the model and experimental technique are appropriate for this catalytic system. Further evidence is obtained by comparison with available literature data on o-xylene isomerization. Ward and Hansford (1969) performed o-xylene isomerization on the H^+ form of ultrastable faujasite and obtained a first-order kinetic rate constant of 0.81 s^{-1} at 533 K for the depletion of o-xylene. This compares favorably to the value of 0.72 s^{-1} at 523 K determined in this study. Ward and Hansford also observed a lack of diffusion resistance in their catalysts by using the method of varying crystallite sizes. Gajewski and Sulikowski (1978) performed o-xylene isomerization on H-USY, and while intrinsic reaction rate constants were not reported, an activation energy of 125.5

Table 3. Heat of Absorption and Activation Energy for Each Ion-exchanged Faujasite

	H-USY	Li-USY	Na-USY
ΔH, kJ/mol	−84.5	−57.7	−31.4
E_a kJ/mol	121.2	84.9	53.5

kJ/mol was determined, which agreed closely with the value of 121.3 kJ/mol observed in this analysis.

No literature data could be found on the ion exchange forms but it was possible to rationalize the results with a theoretical understanding of the zeolite-reactant interaction. Since the adsorptive and catalytic strengths of the zeolite's active sites are believed to be proportional to the charge density (charge/distance) of the site, the cation valence and ionic radius (e^-/r) are then the important parameters governing the zeolite-adsorbate interaction. For the series of ions used in this study one would expect a decrease in catalytic activity and heat of adsorption from H^+, Li^+, Na^+ to K^+, as this is the trend of increasing ionic radius at constant valence. This decrease in catalytic activity was indeed observed by comparing the reaction rate constant at the one temperature (523 K) common to each ion-exchanged form. It was seen that H-USY (0.72) > Li-USY (0.0267) > Na-USY (0.00861) > K-USY (no reaction). This trend would be observed at all the temperatures at which reactions were performed if the Arrhenius expressions were used to extrapolate to different temperatures.

The expected decrease in adsorptive strength was also observed by examining the heat of adsorption for each ion exchange form: H-USY (−84.5) > Li-USY (−57.5) > Na-USY (−31.4). However, observations of the trend in K_a at the common temperature of 523 K showed the reverse order, H-USY (116) < Li-USY (1523) < Na-USY (2567), thus indicating that the surface coverage of reactant in the adsorbed phase increased with ionic radius. This effect was more likely due to competitive adsorption of product since the more active catalyst (H-USY) produced more product (meta- and para- isomers), which was then available to compete with the orthoxylene for adsorption on active sites. Some evidence can be found to support the effect of competitive adsorption by comparing the different catalysts at similar conversion levels. This analysis reveals that similar K_a values are obtained for each ion-exchanged form when compared at constant conversion levels; a rough proportionality between K_a and conversion is also observed (see Supplementary Material).

It was also noted that the activation energy trend with cation exchange (H-USY > Li-USY) > Na-USY) was unusual since from the classical definition of activation energy it would be postulated that the most active catalyst (H-USY) would have the lowest energy barrier for reaction. However, in the presence of heat of adsorption effects this trend in activation energy is often observed. Ashmore (1963) reviewed cases in the literature in which the activation energy decreases with heat of adsorption. He postulated that molecules which are strongly adsorbed (high heat of adsorption) would require a greater amount of energy to react.

Reactions with ZSM-5 and silicalite

Orthoxylene isomerizations were performed on ZSM-5 and silicalite catalysts; typical characteristic functions I and I' are shown for ZSM-5 in Figures 7 and 8. Values for I'' determined for ZSM-5 and silicalite, shown in Table 4, were clearly nonzero, indicating that some diffusion resistance existed. However, reproducibility of I'' values was very poor due to experimental error in the determination of the second moment and no linear relationship with inverse flow rate was observed. The source of error is due to the fact that the definition of I'', Eq. 10, is the difference between two numerically large numbers, M_1^2/M_0^3 and

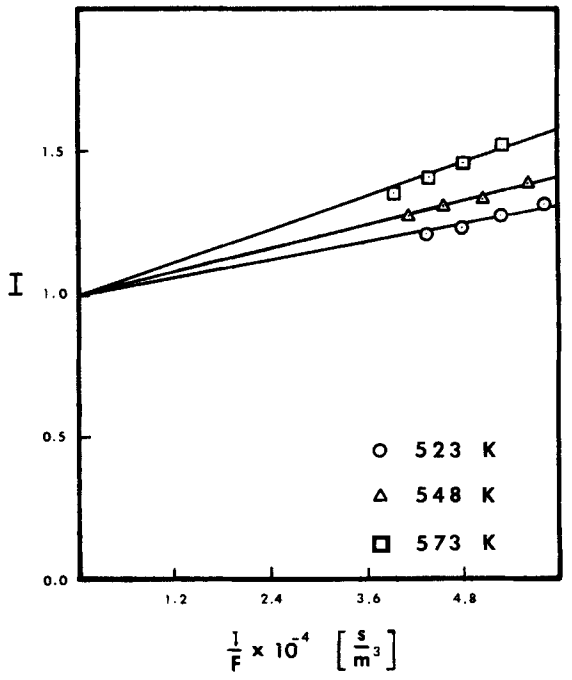

Figure 7. Function I vs. $1/F$ for H-ZSM5.

M_2/M_0^2, while the value of this difference is of similar magnitude as the experimental error. The determination of the second moment was especially error prone because of the importance of the o-xylene concentration values at long times (the "tail" of the reactor effluent response). The tail of the concentration curve was often estimated by an exponential extrapolation from the last few data points, and while this extrapolation had little effect on I and I', the measurement of I'' was affected. Experimental determination of o-xylene concentration at long times was not

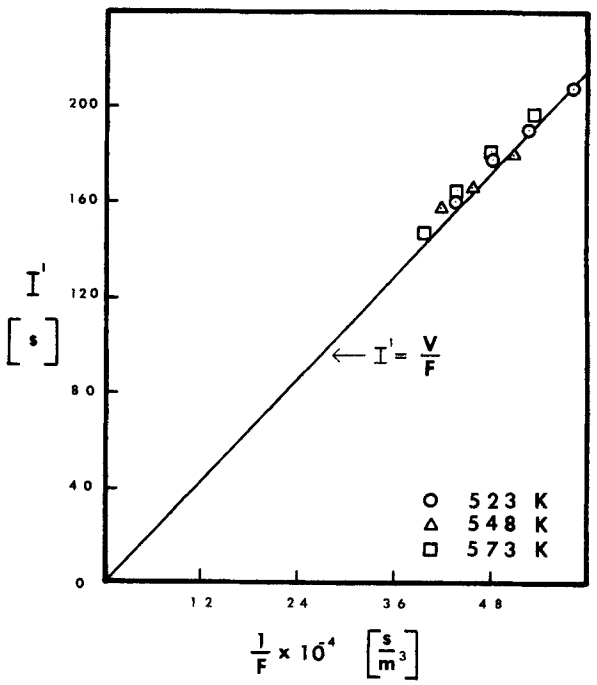

Figure 8. Function I' vs. $1/F$ for H-ZSM5.

Table 4. Typical I'' Values for Silicalite and ZSM-5

Temp. K	Silicalite	ZSM-5
523	—	1,400
548	3,000	—
573	700	—

possible as small amounts of high-boiling impurities (gasket materials and decomposition products) began to elute from the GC columns, thus disturbing the baseline. In some instances, values for I'' could be estimated by taking statistical averages from multiple runs; these data appear in Table 4.

Difficulty in determining K_a from I' plots was also encountered. As shown in Figure 8, all values of I' measured for *ZSM*-5 lie on the reactor residence time locus and similar results were obtained for silicalite. This indicates that the time the reactant spends adsorbed on the zeolite, denoted by the second term in the definition of I', Eq. 9, is not significantly greater than the reactor space time. It is possible that this is due to the high Si/Al ratio of ZSM-5 and silicalite, which provides few adsorption sites; this may also be exacerbated by the existence of concentration gradients within the zeolite crystal, which would reduce access of reactant to adsorption sites in the crystal's interior (effectiveness factor <1.0).

Since K_a could not be determined from I' values, independent experiments were used. Orthoxylene adsorption on silicalite was studied by Wu et al. (1983) and K_a was determined from their sorption uptake curves, while Kokotailo et al. (1981) studied xylene adsorption on ZSM-5, allowing K_a to be calculated from their isotherms. Both studies were performed at low temperatures, so the Van't Hoff law was used to extrapolate to the reaction temperatures of this study. The values of K_a at the corresponding reaction temperatures are shown in Table 5.

With these values of K_a, the expressions for I and I'' were solved by trial and error for the model parameters k_s, D_i, ϕ_i, and η_i, Table 6.

Due to the small values of I'' (relative to the experimental error) it was only possible to calculate reliable parameters for ZSM-5 at one temperature, so values of heat of adsorption and activation energy are not available. These data exist for silicalite, however, and the reaction rate constant and diffusivity were extrapolated by an Arrhenius relationship to the temperature at which ZSM-5 was analyzed. A reaction rate constant for silicalite of 9.05×10^{-4} s^{-1} was calculated at 523 K. This was less than the value for ZSM-5, as was expected, due to the greater concentration of active sites in ZSM-5.

The diffusivity of silicalite can also be extrapolated this way, and a value of 9.8×10^{-13} m^2/s was found at 523 K. This compared, within an order of magnitude, to the value calculated for ZSM-5 (3.55×10^{-13} m^2/s); this is considered an adequate agreement due to the large errors (50%) normally associated with zeolitic diffusivities. One would expect ZSM-5 and silicalite to have similar diffusivities due to their isostructurality. Silicalite's diffusivity can also be extrapolated to room temperature to compare to the value obtained by Wu et al. of 2.2×10^{-16} m^2/s. The value of 8.15×10^{-16} m^2/s thus calculated again compared to within an order of magnitude.

Table 5. K_a for Silicalite and ZSM-5 from Literature Values

Temp. K	Silicalite	ZSM-5
523	—	3,827
548	2,292	2,959
573	1,882	2,339
598	1,614	—

Table 6. Model Parameters for Silicalite and ZSM-5

	Silicalite		ZSM-5
	548 K	573 K	523 K
k_s, 1/s	2.93×10^{-3}	8.56×10^{-3}	8.21×10^{-3}
K_a	2,292	1,882	3,827
D_i, m^2/s	1.48×10^{-12}	2.16×10^{-12}	3.55×10^{-13}
η_i	0.65	0.55	0.5
ϕ_i	3.2	4.1	4.7

Conclusions

Orthoxylene isomerization reactions were performed on four ion-exchange forms (H^+, Li^+, Na^+, K^+) of ultrastable faujasite powder using a gradientless reactor system. No diffusion resistance was observed in the temperature range of 463 to 573 K and none was expected based on previous studies and preliminary calculations. The kinetic rate constant and activation energy determined for the H^+ form of ultrastable faujasite agreed well with available literature values. The decrease in reaction rate and heat of adsorption observed in the ion-exchanged series H^+, Li^+, Na^+, K^+ was explained by the decrease in site charge density that occurs with increasing ion radius. The agreement of the model parameters with the data of previous workers, and also with the theory of active sites in zeolites, provides significant evidence that the model and experimental apparatus used are effective tools in the investigation of reaction and adsorption in porous catalysts.

Data from o-xylene isomerizations performed with silicalite and ZSM-5 catalysts indicated that diffusion resistance was present. The second moment was estimated in these cases using exponential curve fits and averaging multiple runs. The adsorption equilibrium constant could not be determined from the first moment data because the adsorption extent was not sufficient to increase reactant residence time above the reactor space time. This was attributed to both the comparative lack of adsorption sites in ZSM-5 or silicalite relative to faujasite and to the presence of concentration gradients in the crystallite, which would reduce the number of sites accessible to the reactant (effectiveness factor <1.0). Literature values for adsorption equilibrium constant were used in the mathematical model to allow calculation of the reaction rate constant and diffusion rate constant. ZSM-5 showed increased reactivity over silicalite due to the higher concentration of active sites, whereas diffusion coefficients were similar within an order of magnitude, which was attributed to the identical crystal structures of the two catalysts.

The difficulties encountered in measuring the diffusion coefficient were not due to any inherent deficiency in the method of analysis since the expected lack of diffusion resistance was observed in the faujasite-catalyzed reactions. The gradientless reactor and method of moments have also been succsssfully applied to cyclopropane isomerization by Ma and Schobert (1981), in which diffusion coefficients were determined from second moment measurements. However, the applicability of the gradientless reactor technique to more complex chemical

systems, such as structurally similar isomers, can be limited in diffusion-controlled regimes unless adequate analytical techniques are used.

Acknowledgment

The authors thank Mobil Oil Corporation, Union Carbide Corporation, and W. R. Grace, Davison Division, for supplying the catalyst materials used in this study.

Notation

A_v = surface area/volume, m^{-1}
C = concentration, mol · m^{-3}
D = diffusivity, $m^2 \cdot s^{-1}$
E_a = energy of activation, kJ · mol^{-1}
F = gas molar flow rate, $m^3 \cdot s^{-1}$
ΔH = heat of adsorption, kJ · mol^{-1}
I = characteristic function
k_a = adsorption rate constant, s^{-1}
$K_a = K_p A_v/\epsilon_i$ = dimensionless equilibrium constant
$K_p = C_{si}/C_i$ = equilibrium constant, m
k_s = reaction rate constant, s^{-1}
k_{sO} = preexponential factor, s^{-1}
M_i = ith moment of reactor response
N = number of particles or an integer increment
r = radial distance, m
R = particle radius, m
S = Laplace dummy variable
t = time, s
V = reactor volume, m^3
v_i = intracrystalline volume, m^3
X = inlet concentration, mol · m^{-3}
Y = gas phase concentration at effluent, mol · m^{-3}

Greek letters

ϵ = void volume fraction
η = effectiveness factor = $(3/\phi_i^2)(\phi_i \coth \phi_i - 1)$
ϕ_i = modified Thiele modulus = $(R_i K_a k_s/D_i)^{1/2}$
τ = residence time (volume/flow rate), s^{-1}

Subscripts

i = intracrystalline region
0 = at time = 0
a = species a
c = based on concentration
si = based on surface concentration

Literature cited

Ashmore, P. G., *Catalysis and Inhibition of Chemical Reactions*, Butterworths, London, 184 (1963).
Barrer, R. M., "The Properties and Applications of Zeolites," The Chem. Soc. R. P. Townsend, ed., London 4 (1980).
Bassett, D. W. and H. W. Habgood, *J. Phys. Chem.*, **64**(6), 769 (1960).
Bartley, B. H., H. W. Habgood, and Z. M. George, *J. Phys. Chem.*, **72**(5), 1689 (1968).
Breck, D. W., *Zeolite Molecular Sieves*, Wiley, New York 593 (1974).
Brian, P. L. T., and H. B. Hales, *AIChE J.*, **15**, 419 (1969).
Brisk, M. C., R. L. Day, M. Jones, and J. B. Warren, *Trans. Inst. Chem. Eng.*, **46**, T3 (1968).
Carberry, J. J., *Ind. Eng. Chem.*, **56**(11), 39 (1964).
Chiang, A., Ph.D. Diss. Worcester Polytech. Inst. (1982).
Choudary, V. R., and L. K. Doraiswamy, *Ind. Eng. Chem. Process Des. Dev.*, **11**(3), 420 (1972).
Gajewski, F., and B. Sulikowski, *React. Kinet. Catal. Lett.*, **9**(4), 395 (1978).
Kokotailo, G. T., S. L. Lawton, D. H. Olsen, and W. M. Meier, *J. Phys. Chem.*, **85**, 2238 (1981).
Ma, Y. H., and C. Mancel, *AIChE J.*, **18**(6), 1148 (1972).
Ma, Y. H., and M. Schobert, *J. Catal.*, **70**, 102 (1981).
Santacesaria, E., M. Morbidelli, P. Danise, M. Mercenari, and S. Corra, *Ind. Eng. Chem. Process Des. Dev.*, **21**, 440 (1982).
Savage, L. A., Masters Thesis, Worcester Polytech. Inst. (1983).
Ward, J. W., and R. C. Hansford, *J. Catal.*, **13**, 316 (1969).
Wu, P. D., A. Debebe, and Y. H. Ma, *Zeolite*, **3**, 119 (1983).

Manuscript received Aug. 4, 1986, and revision received Feb. 6, 1987.

See NAPS document no. 04512 for 7 pages of supplementary material. Order from NAPS c/o Microfiche Publications, P.O. Box 3513, Grand Central Station, New York, NY 10163. Remit in advance in U.S. funds only $7.75 for photocopies or $4.00 for microfiche. Outside the U.S. and Canada, add postage of $4.50 for the first 20 pages and $1.00 for each of 10 pages of material thereafter, $1.50 for microfiche postage.